Research Article

Journal of Molecular Recognition

Received: 28 October 2009, Revised: 27 December 2009, Accepted: 28 December 2009, Published online in Wiley Online Library: 29 April 2010

(wileyonlinelibrary.com) DOI:10.1002/jmr.1023

# Mechanistic and kinetic characterization of hepatitis C virus NS3 protein interactions with NS4A and protease inhibitors

Matthis Geitmann[a†], Göran Dahl[a‡] and U. Helena Danielson[a*]

**The mechanism and kinetics of the interactions between ligands and immobilized full-length hepatitis C virus (HCV) genotype 1a NS3 have been characterized by SPR biosensor technology. The NS3 interactions for a series of NS3 protease inhibitors as well as for the NS4A cofactor, represented by a peptide corresponding to the sequence interacting with the enzyme, were found to be heterogeneous. It may represent interactions with two stable conformations of the protein. The NS3–NS4A interaction consisted of a high-affinity ($K_D = 50$ nM) and a low-affinity ($K_D = 2$ μM) interaction, contributing equally to the overall binding. By immobilizing NS3 alone or together with NS4A it was shown that all inhibitors had a higher affinity for NS3 in the presence of NS4A. NS4A thus has a direct effect on the binding of inhibitors to NS3 and not only on catalysis. As predicted, the mechanism-based inhibitor VX 950 exhibited a time-dependent interaction with a slow formation of a stable complex. BILN 2061 or ITMN-191 showed no signs of time-dependent interactions, but ITMN-191 had the highest affinity of the tested compounds, with both the slowest dissociation ($k_{off}$) and fastest association rate, closely followed by BILN 2061. The $k_{off}$ for the inhibitors correlated strongly with their NS3 protease inhibitory effect as well as with their effect on replication of viral proteins in replicon cell cultures, confirming the relevance of the kinetic data. This approach for obtaining kinetic and mechanistic data for NS3 protease inhibitor and cofactor interactions is expected to be of importance for understanding the characteristics of HCV NS3 functionality as well as for anti-HCV lead discovery and optimization.** 

**Keywords:** hepatitis C virus; NS3; NS4A; protease; biosensor; SPR; inhibition

## INTRODUCTION

More than 120 million people are currently infected with hepatitis C virus (HCV), but most patients can expect little benefit from the current treatment which has a low cure rate and serious side effects (for reviews, see Feld and Hoofnagle, 2005; Shepard *et al*., 2005). Studies of HCV enzymes suitable as targets for direct antiviral treatment, and subsequent design of potent inhibitors against these, have resulted in a number of promising drug candidates (for a review, see Rönn and Sandström, 2008). One such target is the non-structural protein 3 (NS3), a bifunctional protein with a protease and a helicase function. The protease is a serine protease with a chymotrypsin like fold. It is responsible for the proteolytic processing of the viral polyprotein (Eckart *et al*., 1993) while the helicase/ATPase is responsible for the unwinding of the double stranded viral RNA (Kim *et al*., 1995). In order to be fully folded and active, NS3 needs to be stabilized by an interaction with the viral NS4A cofactor protein. Since the activation of NS3 only requires the central part of this protein, *in vitro* experiments are often performed without the membrane spanning *N*-terminal part which anchors the complex to the membrane *in vivo* (Failla *et al*., 1994; Tomei *et al*., 1996).

HCV drug discovery involving NS3 has predominantly been directed towards its protease activity. The work is typically initially guided by enzyme inhibition analysis, and later by a cell culture system involving the replication machinery of the virus, a 'replicon' (Lohmann *et al*., 1999). The first approach is important since it allows the quantification and characterization of inhibition of the enzyme itself. However, it requires the use of suitable substrate and cofactor analogues, as well as conditions optimized for sensitive and reliable measurements of enzyme activity. Despite the apparent simplicity as compared to cell assays, the requirement of a catalytically active enzyme puts restraints on the assay conditions that can be used and the range of experiments that can be performed. Furthermore, quantification of inhibition is either performed with substrate analogues (e.g. using fluorescence resonance energy transfer

* *Correspondence to: U. H. Danielson, Department of Biochemistry and Organic Chemistry, Uppsala University, BMC, Box 576, 751 23 Uppsala, Sweden. E-mail: helena.danielson@biorg.uu.se*

a *M. Geitmann, G. Dahl, U. H. Danielson Department of Biochemistry and Organic Chemistry, Uppsala University, BMC, Box 576, 751 23 Uppsala, Sweden*

† *Present address: Beactica AB, Box 567, 751 22 Uppsala, Sweden.*

‡ *Boehringer-Ingelheim RCV GmbH & Co KG, Dr. Boehringer-Gasse 5-11, A-1121 Vienna, Austria.*

**Abbreviations:** *HCV, hepatitis C virus; NS3, non-structural protein 3; SPR, surface plasmon resonance; FRET, fluorescence resonance energy transfer; DTT, dithiothreitol; DMSO, dimethyl sulfoxide; MES, 2-(N-morpholino)ethanesulfonic acid; HEPES, 4-(2-hydroxyethyl)-1-piperazineethanesulfonic acid.*

 

(FRET) detection) or involves laborious end-point assays. Even for well-validated procedures, the resulting inhibition constant ($K_i$), that is ideally obtained, is not very informative, since it only provides equilibrium-based information for the inhibition under the conditions used for analysis. Moreover, the kinetic and thermodynamic details or the effect of modified experimental conditions (chemodynamic analysis) on the inhibitor–enzyme interaction cannot be obtained by this approach. Therefore, the drawbacks of multi-component activity-based assays call for alternative analytical approaches with reduced complexities in order to reliably evaluate the detailed characteristics of inhibitors in drug discovery campaigns.

Direct binding assays using surface plasmon resonance (SPR) biosensor technology are suitable complements to inhibition measurements (Huber and Mueller, 2006). We have previously used this technology for studies of inhibitor interactions with a variety of drug targets (Markgren *et al*., 2002; Geitmann and Danielson, 2004; Shuman *et al*., 2004a; Backman *et al*., 2006; Geitmann *et al*., 2006; Nordström *et al*., 2008) in order to characterize the kinetic and mechanistic features of the interactions. The primary advantage of this methodology is that the kinetic mechanism can be determined and the corresponding association ($k_{on}$) and dissociation rate constants ($k_{off}$) can be estimated, thus resolving the equilibrium dissociation constant of the interaction ($K_D$) into its individual rate constants ($K_D = k_{off}/k_{on}$). For more complex mechanisms than a simple 1:1 interaction, it is sometimes possible to determine additional kinetic parameters. In addition, since the detection is substrate independent and conditions do not need to be optimized for high enzyme activity, it is possible to use a wide range of conditions so that the characteristics of interactions can be extensively explored.

In order to obtain a direct binding assay for studying inhibitor and cofactor interactions with HCV NS3, an SPR-based biosensor assay for full-length NS3 from genotype 1a was developed. It was used to characterize the interaction between NS3 and NS4A, and several protease inhibitors varying in structure and inhibitory potencies (Figure 1). Notably, compounds previously or currently tested in the clinic were included. ITMN-191 is a potent peptidomimetic macrocyclic inhibitor (Seiwert *et al*., 2008), similar to BILN 2061 (Llinàs-Brunet *et al*., 1998), but different to VX-950, which is a linear mechanism-based inhibitor (Summa, 2005). By measuring interactions with a surface where NS3 alone was immobilized, in parallel with a surface where NS3 was co-immobilized with NS4A, the effect of the cofactor on inhibitor interaction with NS3 could be investigated. The kinetic parameters for a series of NS3 inhibitors were successfully determined and found to correlate well with inhibition data from an activity-based inhibition assay as well as from a viral replication-based assay, thus validating the assay and confirming

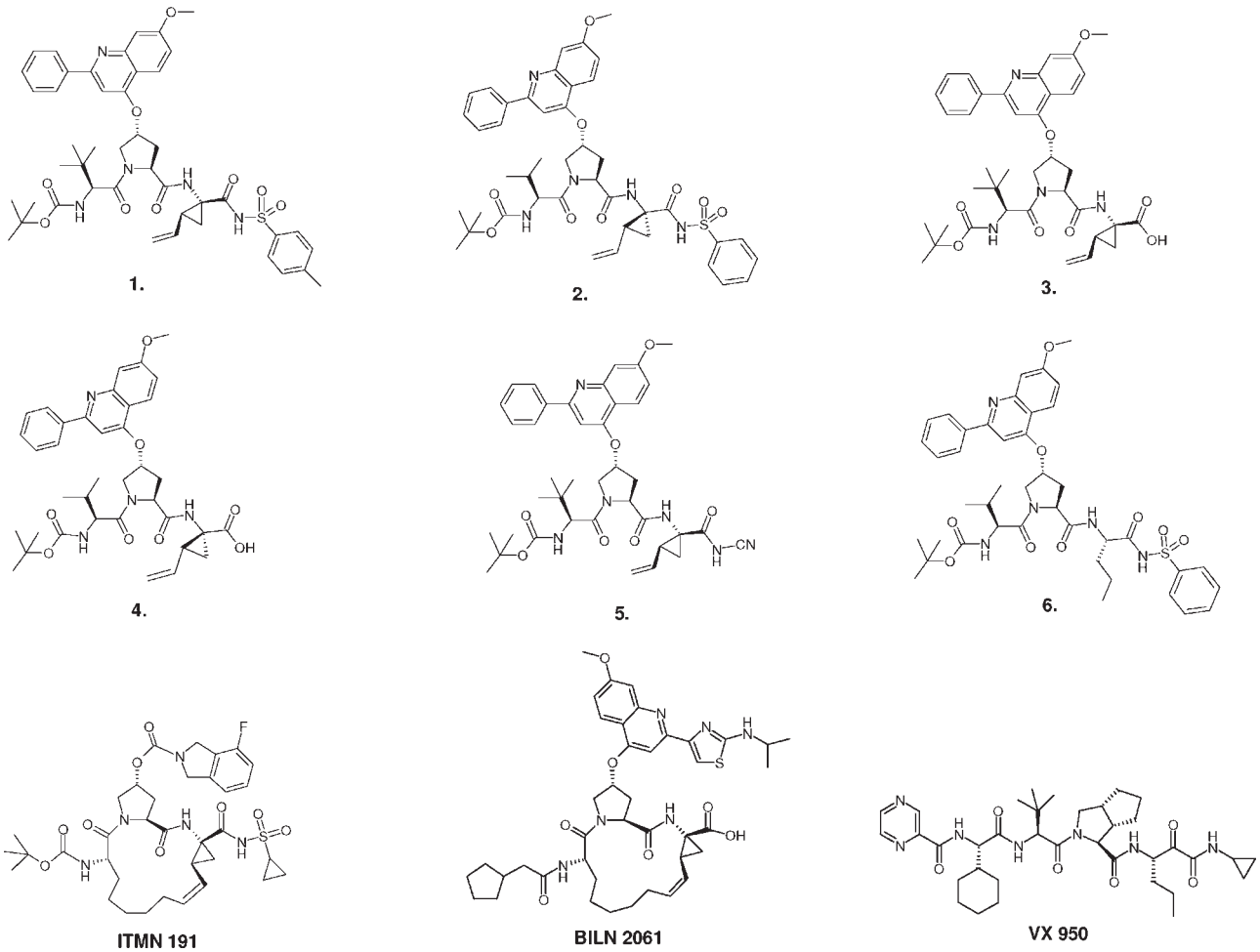


**Figure 1.** Structures of the studied inhibitors.



  

that the data is relevant for HCV drug discovery. In addition, new mechanistic details and complexities in the interactions were revealed.

## MATERIALS AND METHODS

### Enzyme, cofactor and inhibitors

Expression and purification of full-length NS3 from HCV genotype 1a was performed as described previously (Poliakov *et al*., 2002; Dahl *et al*., 2007a, b). The NS4A cofactor peptide (KKGSVVIVGRIVLSGK), denoted NS4A throughout the paper, was synthesized according to published procedures (Poliakov *et al*., 2002). It was a kind gift from Gunnar Lindeberg, the Department of Organic Pharmaceutical Chemistry, Uppsala University, Uppsala, Sweden. Inhibitors 1–6 were synthesized according to published protocols (Rönn *et al*., 2006, 2007). BILN 2061 was obtained from Boehringer Ingelheim and VX 950 from the VIRGIL DrugPharm Team. ITMN-191 was synthesized according to published procedures (International Publication Number WO 2005/037214 A2, Compound AR00334191).

### Interaction kinetic analysis

All interaction experiments were performed with a BIAcore 2000 SPR biosensor instrument, CM5 or CM7 sensor chips, and standard reagents for immobilization (GE Healthcare Life Sciences, Uppsala, Sweden). For immobilization to CM5 sensor chips, aliquots of 200 μl NS3 at 0.1 mg/ml were subjected to buffer change into immobilization buffer (50 mM MES pH 6.0 (Sigma–Aldrich Sweden AB, Stockholm, Sweden), 0.1% *n*-octyl-β-D-glucopyranoside (Anatrace, Maumee, OH, USA) and 4 mM DTT (Sigma–Aldrich Sweden AB, Stockholm, Sweden)) and concentrated to 50 μl, 0.4 mg/ml, using YM-30 micro spin columns (Millipore AB, Nödinge, Sweden). For immobilization to the CM7 sensor chip, the enzyme was only subjected to a buffer change (i.e. without concentrating the enzyme), using the immobilization buffer above and Pierce protein desalting spin columns (VWR, Stockholm, Sweden).

The enzyme was immobilized by amine coupling to activated CM5 or CM7 chip surfaces, as recommended by the manufacturers. For co-immobilization of the NS3–NS4A complex, 100 μM NS4A, dissolved in 50 mM HEPES (Sigma–Aldrich Sweden AB, Stockholm, Sweden), pH 7.4, 3% DMSO (Sigma–Aldrich Sweden AB, Stockholm, Sweden), was injected for 3 min over one of the NS3 surfaces and an empty activated surface prior to a deactivation using ethanolamine, or 20 mM Tris-HCl, pH 7.4 (Sigma–Aldrich). The deactivation was required since NS4A contains primary amines that can react with the surface if the peptide is injected as an analyte over a surface that still contains reactive groups. This procedure resulted in surfaces with NS3 alone, NS3 and NS4A together, and NS4A alone (Figure 2).

Interaction experiments were typically performed at 25°C with 50 mM HEPES, pH 7.4, 0.1% *n*-octyl-β-D-glucopyranoside (Anatrace, Maumee, OH, USA), 2 mM DTT and 3% (v/v) DMSO as running buffer and a flow rate of 50 μl/min. The interaction between immobilized NS3 and NS4A injected as analyte was investigated using a concentration series of NS4A, ranging from 15.6 nM to 1 μM. The peptide was diluted in running buffer and injected for 60 s over the NS3 surface.

Inhibitors were typically prepared as 4-fold dilution series from 5 μM to 5 nM. The compounds were diluted in running buffer and injected for 60 s over the surfaces. The analysis of time-dependent interactions with NS3 was performed with VX 950, BILN 2061 and ITMN-191, using a series of injection times from 30 to 500 s.

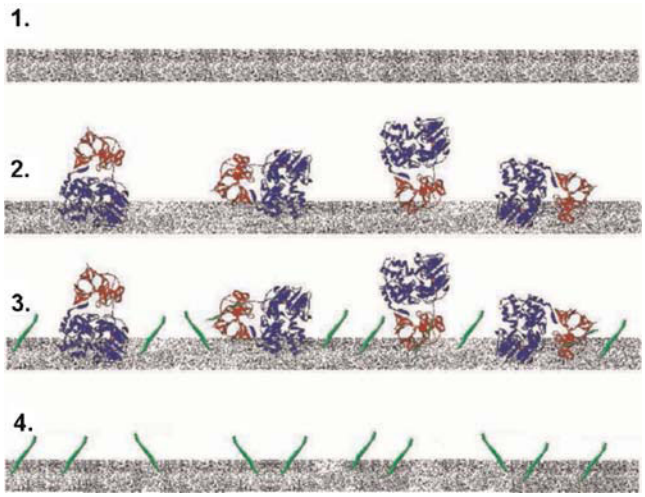


**Figure 2.** Cartoon of the four biosensor surfaces used for the interaction studies: (**1**) blank (i.e. unmodified dextran matrix), (**2**) full-length NS3, (**3**) full-length NS3 and NS4A (co-immobilized), (**4**) NS4A. The NS3 protease domain is shown in red and the helicase domain in blue (based on PDB: 1CU1 (Yao *et al*., 1999)), the NS4A peptide is shown in green.

Analysis of the sensorgrams was performed using BiaEvaluation software 3.0 (GE Healthcare Life Sciences). Sensorgrams from the reference surfaces and blank injections were subtracted from the raw data. Kinetic parameters of the interactions were determined by global analysis of series of corrected sensorgrams at different analyte concentrations, using an equation representing a 1:1 binding model including a term for bulk effects and a drifting baseline where necessary. A two-step binding model ('two-state reaction' according to the BiaEvaluation software terminology) without bulk correction was used to determine the kinetic parameters for VX 950 from sensorgrams with an association phase of 5 min. A double exponential model ('heterogeneous ligand — parallel reactions') without bulk correction was used to determine the kinetic parameters for ITMN-191 and BILN 2061, and for the NS3–NS4A interaction.

### Inhibition analysis

Inhibition measurements using a steady-state enzyme activity assay were performed as described previously (Dahl *et al*., 2007a, b); 1 nM NS3 was pre-incubated with 25 μM NS4A and varying inhibitor concentrations in assay buffer (50 mM HEPES pH 7.4, 40% (w/v) glycerol, 0.1% (w/v) *n*-octyl-β-D-glycopyranoside and 10 mM DTT, 3.33% (v/v) DMSO) for 10 min at 30°C. The reaction was started by addition of 0.5 μM substrate (Ac-Asp-Glu-Asp(EDANS)-Glu-Glu-Abu-ψ-[COO]Ala-Ser-Lys(DABCYL)-$NH_2$ (RET S1, AnaSpec, San Jose, CA, USA)). The initial rates were fitted to an equation for competitive inhibition, or tight-binding competitive inhibition (Dahl *et al*., 2007a), using nonlinear regression analysis (STATISTICA, StatSoft Inc., Tulsa, OK, USA). A correlation analysis between $K_i$ and $k_{on}$, $k_{off}$ or $K_D$ values obtained using a surface with NS3 or NS3 with NS4A, and with



 

Journal of Molecular Recognition

data from published replicon inhibition analysis (Lin *et al*., 2004; Rönn *et al*., 2006, 2007) was also performed with STATISTICA.

## RESULTS

### Development of interaction analysis assay

Immobilization of full-length HCV NS3 (Mw = 72 000 Da) to CM5 sensor chips resulted in surface densities around 4000 RU, while immobilization of NS4A (Mw = 1600 Da) resulted in levels around 1 500 RU. The level of NS4A immobilized to the surface where NS3 was already immobilized was comparable to the levels obtained when immobilizing NS4A to an empty surface. The apparent binding capacity of the NS3 surface was low (10–20%), as determined with BILN 2061, and differed between runs. Still, the sensitivity of the surfaces was adequate for most of the experiments and the non-binding fraction did not appear to interfere with the analysis (see below). A small improvement of the binding capacity was seen when changing the deactivating agent from ethanolamine to Tris-buffer. A chemical regeneration of the surfaces after injection of the inhibitors was not performed since none of the regeneration means tested removed the inhibitor without damaging the immobilized protein. The surface was therefore 'regenerated' by simply allowing the compound to dissociate for an extended period. This procedure was also sufficient for removing any non-covalently attached NS4A on the NS3 surface after immobilization.

During the course of this study, the novel CM7 sensor chips were made available. With these, surface densities of up to 12 000 RU and apparent binding capacities of 30–40% could easily be reached with NS3. The higher functionality of the immobilized protein may be a consequence of not having to concentrate the very sensitive enzyme before immobilization. However, as the CM7 chip was introduced late in the experimental phase of this study, it was only used for validation of the kinetics with the most potent compounds and for the time-dependency experiments (see below), requiring the enhanced sensitivity.

### NS3–NS4A interactions

The interaction between NS3 and NS4A was analysed with NS3 immobilized to the CM5 sensor chip and NS4A injected as analyte at different concentrations. It was limited to NS4A concentrations $\leq 1\ \mu M$, where the unspecific binding of NS4A to the negatively charged sensor surface was not observed. The sensorgrams with different NS4A concentrations could best be described by a heterogeneous binding model with a double exponential function (Figure 3). Global fitting revealed a high-affinity interaction with $K_{D1} = 53.2 \pm 18.5$ nM and a low-affinity interaction with $K_{D2} = 2.1 \pm 1.0\ \mu M$. The two interactions contributed approximately equally to the overall signals, as shown in the inset of Figure 3. They differed mainly in their dissociation rate constants ($k_{off1} = 0.0023 \pm 0.0003\ s^{-1}$, $k_{off2} = 0.058 \pm 0.014\ s^{-1}$), rather than in their association rate constants, which were similar ($k_{on1} = 46\,000 \pm 13\,000\ M^{-1}\ s^{-1}$, $k_{on2} = 31\,000 \pm 10\,000\ M^{-1}\ s^{-1}$). (Values are based on three replicates.)

### Inhibitor interactions with NS3

The inhibitor interactions were typically analysed towards four surfaces in parallel: (1) a blank dextran surface, (2) NS3 immobilized alone, (3) NS3 and NS4A co-immobilized and (4) NS4A immobilized alone (Figure 2). Surfaces 1 and 4 served as reference surface for surfaces 2 and 3, respectively, and were used for correction of data. All inhibitors showed a concentration dependent and saturable interaction with the surfaces containing NS3, independent on whether NS4A was immobilized or not (Figure 4). Kinetic parameters were estimated from sensorgrams of 1 min injections using a 1:1 interaction model, except for VX 950 and inhibitor 6. For VX 950, a two-step interaction model was fitted to the data, while a 1:1 model with a drifting baseline was used for inhibitor 6. The drift in this experiment was a result of an incompletely stabilized surface after immobilization, a phenomenon that can affect the baseline of the first sensorgrams recorded with a new surface. The quality of the data obtained in the initial experimental design (using CM5 sensor chips) was not high enough for a more detailed mechanistic and quantitative analysis using a heterogeneous model, as used later (see below). Nevertheless, the kinetic parameters were well enough estimated for a basic SAR analysis and analysis of the effect of NS4A on the interactions. This was facilitated by visualization of the data in an interaction kinetic plot (Figure 5), which shows clear kinetic differences upon minor structural changes in the structures of the compounds and that all compounds bound with higher affinity to the surface containing both NS3 and NS4A than to the surface with NS3 alone. The effect by NS4A on $k_{on}$ and $k_{off}$ varied for different inhibitors, showing that it was dependent on the inhibitor structure. The effect on the affinity was largest for compounds 3 and 5, with 30–40-fold increases, whereas the other inhibitors were affected to a lower degree.

VX 950, which has been proposed to be a slow-binding mechanism-based inhibitor (Summa, 2005), had the slowest association rate constant of all studied compounds for both NS3 surfaces. In order to explore the time-dependency of the interaction and to clearly visualize the effects of the covalent intermediate, an experiment with a series of different injection times was performed (Figure 6). The analysis of the sensorgrams

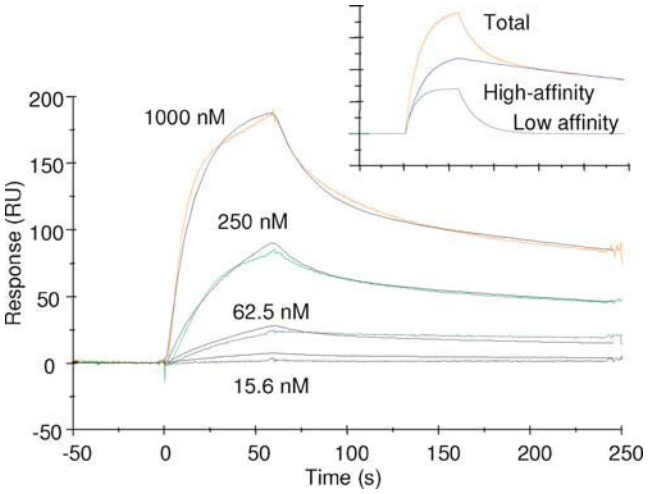


**Figure 3.** SPR sensorgrams for the interaction between NS3 and NS4A. NS3 was immobilized to CM5 sensor chips and NS4A was injected as analyte at the concentrations indicated. Theoretical curves representing the best fit with a heterogeneous binding model (parallel reactions) are overlaid the experimental traces. The inset shows the total binding signal at 1000 nM and the contributions of the high-affinity and low-affinity interactions.



  

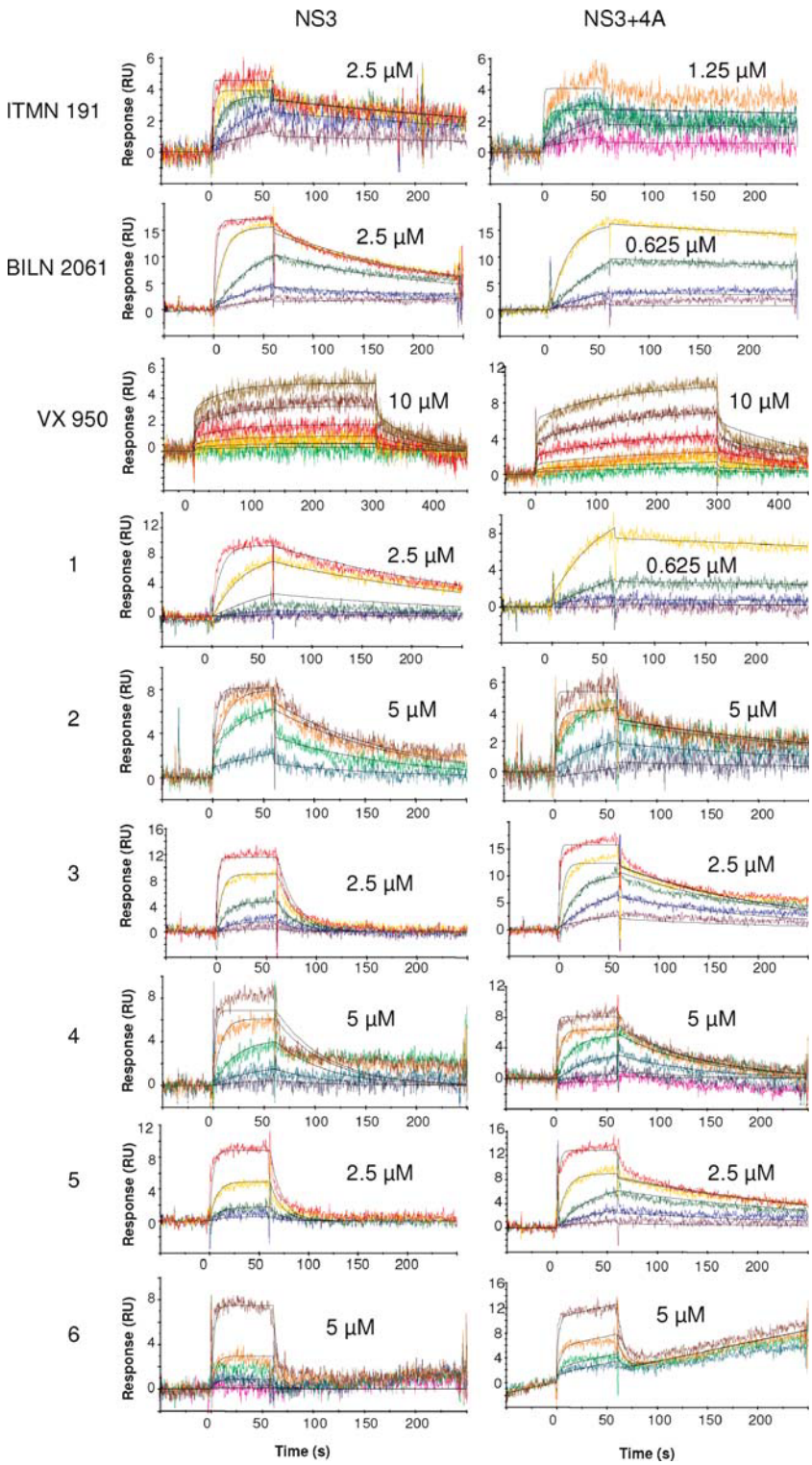


**Figure 4.** SPR sensorgrams for the interaction between inhibitors and immobilized NS3, or co-immobilized NS3 and NS4A. The experiments were performed using a CM5 sensor chip. A 1:1 binding model was fitted globally to sensorgrams of 4-fold dilution series starting from the highest concentration specified in each graph. A two-step model was fitted globally to the sensorgrams of 2-fold dilution series of VX 950. A 1:1 model with drifting baseline was used for compound 6. Theoretical curves (black) are overlaid the experimental traces.

with a two-step model revealed that VX 950 interacted with immobilized NS3 with a $k_{on} = 24\,000\ s^{-1}\ M^{-1}$ and a $k_{off} = 0.52\ s^{-1}$ to form an initial complex, which then reacted with a forward rate $k_1 = 0.016\ s^{-1}\ M^{-1}$ and backward $k_{-1} = 0.015\ s^{-1}$ to give a more stable complex. The parameters were also determined for the NS3/NS4A surface: $k_{on} = 26\,000\ s^{-1}\ M^{-1}$, $k_{off} = 0.41\ s^{-1}$, $k_1 = 0.0084\ s^{-1}\ M^{-1}$, $k_{-1} = 0.0050\ s^{-1}$, showing a stabilizing effect by NS4A. VX 950 was not included in the interaction kinetic graph



 

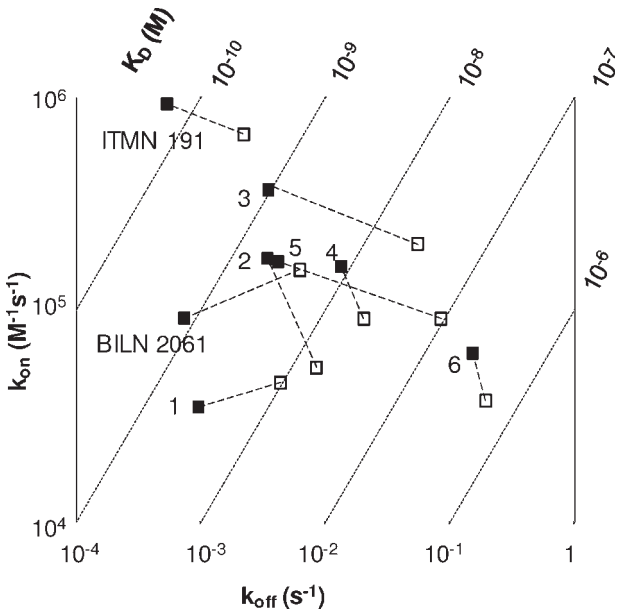


**Figure 5.** Interaction kinetic plot ($k_{on}$ vs. $k_{off}$) for protease inhibitors interacting with NS3. The diagonals represent $K_D$ in M units (the scale is defined above and to the right of the graph). The kinetic parameters were determined by global fit of sensorgrams in Figure 4 using a 1:1 binding model and 60 s injections. Values are shown for the interaction with NS3 alone (□) and with NS3 co-immobilized with NS4A (■). The dashed lines connect the data obtained for a particular inhibitor with the two surfaces.

(Figure 5) since the kinetic parameters for its two-step binding mechanism are not comparable to $k_{on}$ and $k_{off}$ values for a 1:1 interaction.

Since it has been proposed that both ITMN-191 (Rajagopalan *et al*., 2009) and BILN 2061 (Flores *et al*., 2009) interact via a two-step mechanism, an experiment with a series of different injection times was also performed for these compounds. For these experiments, the higher sensitivity of the CM7 sensor chip was exploited. The global analysis of sensorgrams recorded at different concentrations and contact times of BILN 2061 and ITMN-191 revealed that the interactions were heterogeneous and could best be described by a double exponential function (Figure 7). The low-affinity interaction and the high-affinity interaction differed by a factor 10 for BILN 2061 and 15 for ITMN-191 (Table 1). The contributions of the low-affinity (35%) and the high-affinity interaction (65%) to the overall binding signals were similar for both compounds. Regression analysis using a simple 1:1 binding model resulted in similar values for the individual rate constants as determined using CM5 chips, which were between the high and the low-affinity interaction (Table 1). The low-affinity interaction and the high-affinity interaction differed mainly in the dissociation rate constant. A two-step model, as suggested for mechanism-based inhibitors, did not give a better description of the data than the heterogeneous binding model, as judged by calculated $\chi^2$ values. The experiment showed a clear difference in the kinetics for the two compounds. The high affinity interaction of ITMN-191 had an 8-fold lower $K_D$ as a result of both a 4-fold faster association rate and a 2-fold slower dissociation rate. Notably, similar differences in the magnitudes of the low affinity interaction were also observed.

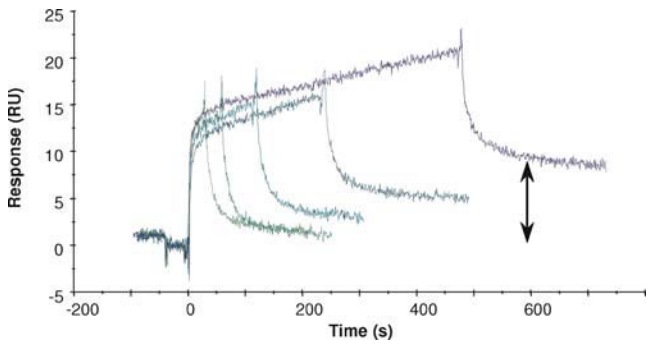


**Figure 6.** The time-dependent binding of VX 950 to NS3. Overlay of sensorgrams for the same inhibitor concentration (20 μM) and different injection times using a CM5 sensor chip. The arrow shows the shift in baseline indicative of a two-step interaction.

### Correlation analysis

A correlation analysis of the kinetic parameters for the inhibitor interactions ($k_{on}$, $k_{off}$, $K_D$) with NS3 alone, as well as together with NS4A, and enzyme inhibition constants ($K_i$) and inhibitory effect in replicons ($EC_{50}$) was performed in order to determine how the interaction kinetic data related to the different types of inhibition data. In order to have a data set with $K_i$-values determined in the same experiment (for example using the same reagents and enzyme batch), the inhibition was determined again specifically for this study. The values were similar to previously determined values, i.e. within 20–30%. Despite the small number of data points, correlations could clearly be distinguished. The analysis revealed that $k_{off}$, $K_D$ and $K_i$ values all had a high correlation with inhibitory effect in replicons, with minor differences (Figure 8). It can thus be concluded that biosensor-based interaction kinetic measurements can be used to predict the potency of compounds in replicon-based cell cultures. The predictability was slightly higher for dissociation rate constants than for $K_D$-values, but did not require NS4A, simplifying the experimental design for this goal. $K_i$-values had a high correlation with $EC_{50}$-values, but a lower correlation with $K_D$-values.

## DISCUSSION

This study has provided a new tool and new information of relevance for HCV drug discovery. By immobilizing full-length NS3 from genotype 1a of HCV on a sensor chip it was possible to determine the kinetic characteristics of protease inhibitors interacting with the protein and also to understand the role of NS4A. Unexpectedly, all studied interactions were found to be heterogeneous, suggesting the presence of at least two stable forms of NS3.

Although the protease functionality of NS3 was in focus, full length NS3 was used despite the increased experimental challenges as compared to when using only the protease domain of truncated NS3. Since the physiological form of NS3 consists of both the helicase and protease domain, and there is now evidence that the helicase domain influences NS3 interactions with NS4A as well as protease inhibitors, it can be considered to be the most relevant form of NS3 for this type of study (Dahl *et al*., 2007a, b; Beran and Pyle, 2008; Beran *et al*., 2009). In contrast, NS4A was used in a truncated form with extra amino acids added to the N- and C-termini for increased



  

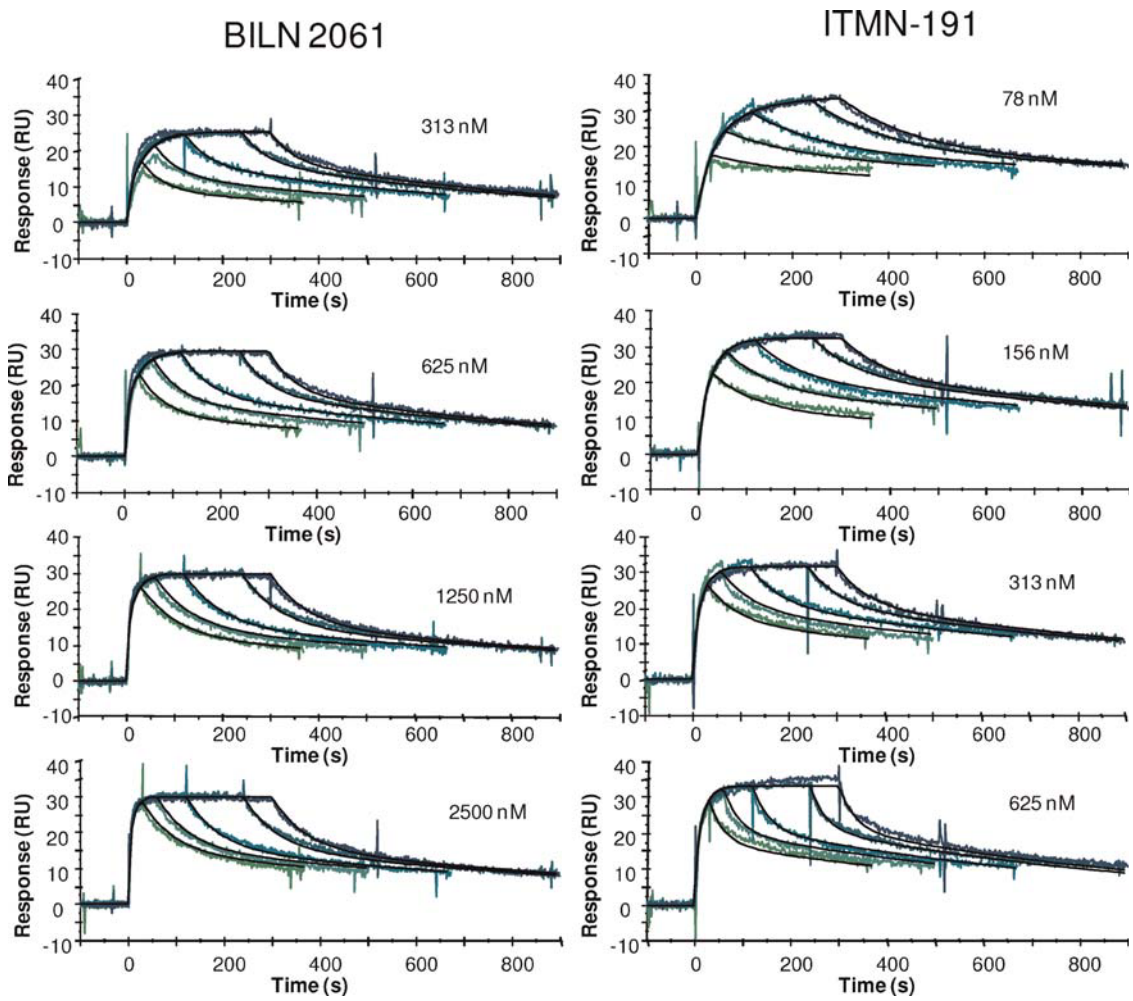


**Figure 7.** The interaction between BILN 2061 and ITMN-191 with NS3 as a function of time and concentration. Sensorgrams with 30, 60, 120, 240 and 300 s injections (from left to right) using a CM7 sensor chip and four different inhibitor concentrations in a 2-fold dilution series with the highest concentration indicated in each graph. A heterogeneous model with drifting baseline was fitted globally to the sensorgrams and the resulting curves are overlaid the experimental traces.

solubility. It has been shown to suffice in other *in vitro* assays for studies of NS3 (Tomei *et al.*, 1996) and avoided the complexities of using the full-length protein that has a membrane binding domain. By not genetically fusing the NS4A peptide to the NS3 protein, as is often done, it was also possible to study the effect of the cofactor on inhibitor interactions.

### Biosensor assay for NS3 protease

A major challenge when developing this biosensor assay has been the poor stability of the NS3 protein. It resulted in large variations between immobilization experiments, despite identical procedures, and it was not stable enough to allow a chemical

**Table 1.** Kinetic constants for interactions between BILN 2061 and ITMN-191, and NS3

| | | | | BILN 2061 | | | ITMN-191 | | |
|---|---|---|---|---|---|---|---|---|---|
| Surface | Chip | Model | Site | $k_{on}$ ($10^5\ M^{-1}\ s^{-1}$) | $k_{off}$ ($10^{-3}\ s^{-1}$) | $K_D$ (nM) | $k_{on}$ ($10^5\ M^{-1}\ s^{-1}$) | $k_{off}$ ($10^{-3}\ s^{-1}$) | $K_D$ (nM) |
| NS3-NS4A | CM5 | 1:1 | | 0.92 | 0.73 | 7.9 | 9.3 | 0.53 | 0.57 |
| NS3 | CM5 | 1:1 | | 1.5 | 6.2 | 40 | 6.7 | 2.2 | 3.3 |
| NS3 | CM7 | 1:1 | | $0.92 \pm 0.19$ | $2.5 \pm 0.6$ | $29 \pm 8$ | $4.9 \pm 2.5$ | $1.6 \pm 0.2$ | $4.0 \pm 1.6$ |
| NS3 | CM7 | Hetero-geneous | High-affinity | $1.5 \pm 1.0$ | $1.6 \pm 0.5$ | $16 \pm 11$ | $4.3 \pm 2.8$ | $0.78 \pm 0.30$ | $2.2 \pm 1.2$ |
| | | | Low-affinity | $1.7 \pm 1.4$ | $21 \pm 8$ | $160 \pm 70$ | $6.1 \pm 4.3$ | $11 \pm 4$ | $32 \pm 34$ |

Values determined using the CM7 chip is presented with standard deviations based on at least four replicates.



 

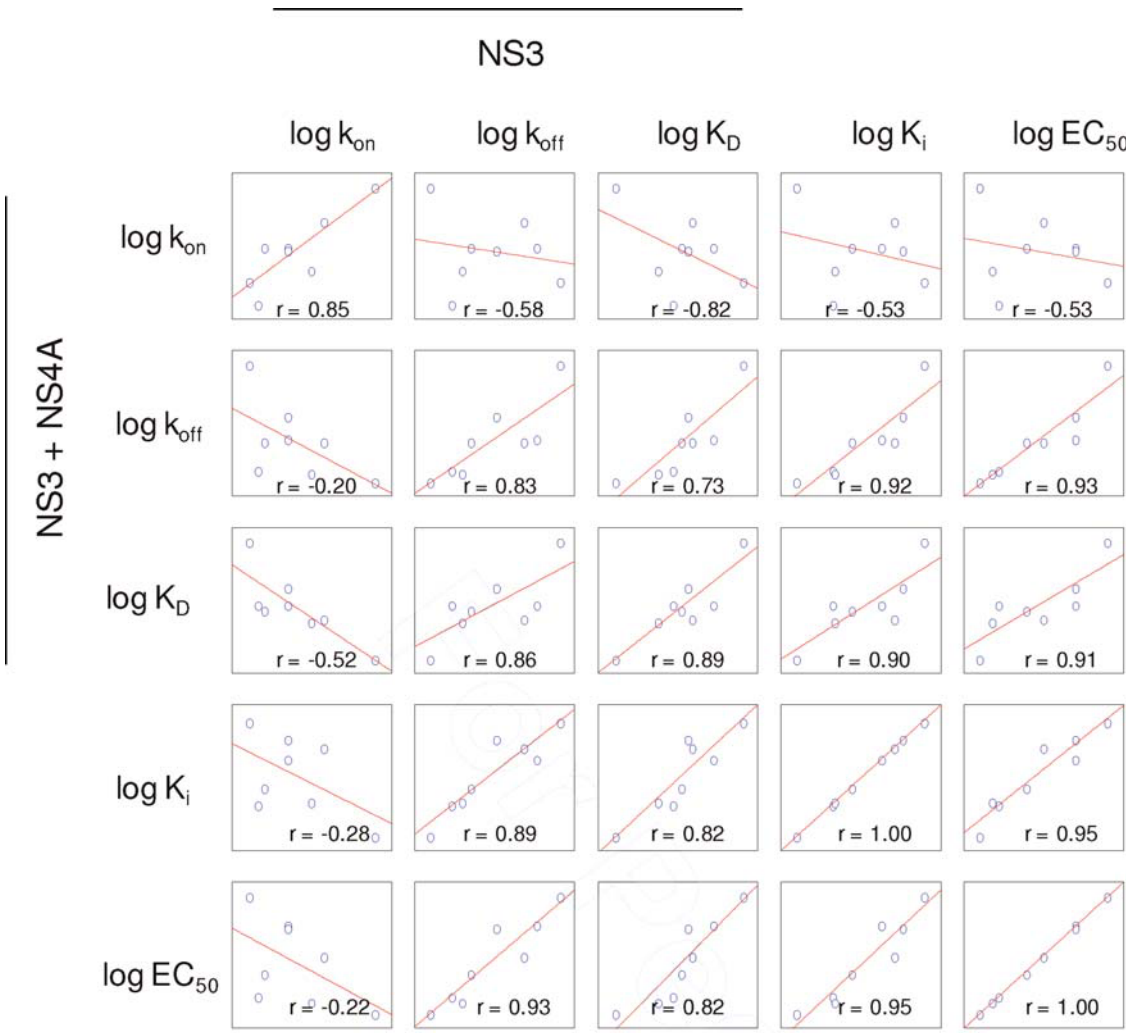


**Figure 8.** Correlation analysis between log $k_{on}$, log $k_{off}$, log $K_D$, log $K_i$ and log $EC_{50}$ for the studied protease inhibitors using CM5 surfaces with only NS3 or NS3 co-immobilized with NS4A. The *r*-value, which is an estimate of the correlation, is shown in the bottom for every graph (*r*-value of 1.0 is 100% correlation). The $EC_{50}$-values were obtained from (Rönn *et al*., 2006) (compounds 1, 3 and 5), (Rönn *et al*., 2007) (compounds 2, 4 and 6), (Lin *et al*., 2004) (BILN 2061) and (Seiwert *et al*., 2008) (ITMN-191). VX 950 was omitted from the analysis due to its two-step binding mechanism.

regeneration of the surface. Nevertheless, it was fairly stable once immobilized and could be used for several days. A second difficulty was a consequence of the low degree of functional protein immobilized on the chip, as compared to the theoretical binding capacity of the immobilized protein (which represents the signal expected at saturation for a compound of known molecular weight and affinity). The small improvement in binding capacity achieved when changing the deactivating agent from ethanolamine to Tris-buffer was possibly due to the lower pH in the Tris buffer (7.5) compared to the ethanolamine (8.5), which avoids exposing the protein to a high pH during this procedure.

During the experimental work, a high capacity sensor chip (CM7) became available. It was specially developed for immobilization of proteins that are challenging to attach covalently to the sensor surface and low molecular weight analytes. Amine coupling of NS3 protein to these new chips resulted in up to 3-fold higher immobilization levels than when using similar protocols with CM5 chips. Furthermore, the apparent functionality of the immobilized protein also increased up to 2-fold. Together, this resulted in much higher and clearer signals for the interactions between inhibitors and NS3. This type of sensor chip is therefore expected to be very useful for further analysis of full-length NS3 interactions and other interactions with low signal levels.

The performance of the biosensor assays was validated using a panel of inhibitors covering a wide range of affinities. The importance of resolving the inhibition constant into the individual rate constants for SAR analysis is illustrated by the broad distribution of compounds in the interaction kinetic plot. Had affinity alone differed upon structural changes, the compounds would have been aligned on a diagonal from the top left corner to the bottom right corner. This shows that $k_{on}$ and $k_{off}$ are not correlated (as also shown in the correlation analysis) but that they provide different information. Consequently, the individual



  

rate constants are important for understanding the structure *kinetic* relationships of interactions, an important part of lead characterization and optimization. This is a major benefit of direct analysis of enzyme–inhibitor interactions as compared to the indirect analysis of enzyme inhibition using an activity-based assay.

The high correlation between the kinetic parameters and the inhibition data, obtained with either an enzyme inhibition assay or replicons in cell culture (see below), confirmed that the determined kinetic parameters were relevant for biological efficacy (i.e., ultimately pharmacokinetics). Interestingly, the dissociation rate constants $k_{off}$ were found to be best correlated with the inhibition constants ($K_i$) and effective concentrations $EC_{50}$. A different relationship was previously reported for HIV-1 protease inhibitors (Shuman *et al*., 2004b), supporting the importance of determining the correlation between individual rate constants and a more physiological assay for each target.

### NS3 and NS4A interactions

One of the aims of this study was to explore the characteristics of the interaction between full length NS3 and NS4A. Although this interaction has been studied extensively previously, the characteristics of the interaction are not clear. This is because the results obtained have been dependent on the method and the different variants of both NS3 and NS4A, and also because the interaction is affected by numerous factors (Bianchi *et al*., 1997; Urbani *et al*., 1999).

This study showed that the interaction between immobilized full length NS3 and the NS4A peptide injected as analyte was in the nanomolar range and that the dissociation was relatively slow. Remarkably, this affinity was much higher (50-fold lower $K_D$) than that obtained with indirect methods based on the measurement of enzyme activity at different NS4A concentrations (Bianchi *et al*., 1997; Poliakov *et al*., 2002). In contrast, based on the extensive interactions between NS3 and NS4A seen in the crystal structure of the complex, the affinity is believed to be in the nanomolar range and not in the micromolar range (Kim *et al*., 1996; Bianchi *et al*., 1997), in line with the new data. An unexpected observation was that the interaction between NS4A and NS3 was heterogeneous. It is possible that differences in affinities for the NS3–NS4A interaction determined in previous studies are a result of significant contributions of multiple/heterogeneous interactions to the analysis. They will contribute to the results even when not explicitly detected. The heterogeneity of the NS4A interactions is discussed further below.

### Interaction kinetic analysis of inhibitors

The interaction between NS3 and a number of protease inhibitors was initially characterized in the presence or absence of the NS4A cofactor peptide. In order to explore the effect of NS4A on inhibitor interactions, the NS4A peptide was co-immobilized with NS3 on the same surface. An alternative experimental design, where the cofactor is pre-injected over NS3 surfaces before injection of inhibitor, was not possible since the complex was too short lived under the conditions used. Considering the high flexibility of the dextran matrix to which the molecules are immobilized, it is reasonable to assume that co-immobilization results in the formation of NS3–NS4A complexes on the chip that are more stable since the local concentration of the two proteins is high. As inhibitors also interacted with immobilized NS4A (data not shown), it was necessary to use two reference surfaces for data analysis; one blank surface and one with only NS4A.

All interaction constants (with the exception for those for VX 950) were initially determined using a simple 1:1 interaction model. However, the model was suboptimal and other interaction models were therefore also evaluated in an attempt to identify more suitable models. In the case of VX 950, it was reasonable to assume that a two-step binding event was involved. However, it was only for VX 950 that the model resulted in a significantly better description of the data than the 1:1 model. As for the interaction between NS4A and NS3, a heterogeneous surface model represented the data well. The high sensitivity of the CM7 enabled experiments that confirmed that the interactions with inhibitors were heterogeneous and that the 1:1 model could be used to determine kinetic constants that were adequate for an initial SAR analysis. (The heterogeneity of the inhibitor interactions is discussed below.)

Consequently, for the analysis of the effect of NS4A on the inhibitor interaction and the correlation analysis with inhibition data, kinetic parameters were extracted using a simple 1:1 model. Facing the suboptimal data quality for some compounds, the reduced number of variables resulted in a more robust and reliable fit. As exemplified for BILN 2061 and ITMN-191, this gave a good approximation of the parameters for the high-affinity interaction. It has been shown that VX 950 is a slow, mechanism-based inhibitor to NS3 (Rajagopalan *et al*., 2009). Despite the limited resolution, a two-step binding mechanism for VX 950 could clearly be seen, in accordance with this proposed model. However, due to the limited data set and major differences in assay methods, the determined rate constants were not readily comparable to those obtained using other methods (Summa, 2005; Flores *et al*., 2009). Still, the biosensor-based assay shows that it can clearly distinguish between the different interaction mechanisms of the different types of inhibitors (i.e. direct reversible, mechanism-based and tight-binding). This presents a valuable alternative experimental approach to previous methods for mechanistic analysis of NS3 protease inhibitors (Poliakov *et al*., 2007), which will aid the development and understanding of new inhibitors and their mode of action.

Two recent studies have also indicated a two-step mechanism for both BILN 2061 (Flores *et al*., 2009) and ITMN-191 (Rajagopalan *et al*., 2009). However, the present study did not support such a mechanism for either BILN 2061 or ITMN-191. There are several potential practical explanations for this discrepancy, for example associated with the different strain variants and constructs of the full-length NS3 used for the experiments, as well as different experimental conditions. Also, the contact time used for interaction analysis versus the pre-incubation time and mixing order used in the more complex substrate-based assays can potentially influence the interpretation of the data. Since the current experimental set up was satisfactory for monitoring the time-dependent interaction between NS3 and VX 950, it appears that neither BILN 2061 nor ITMN-191 can be stated to interact in a time-dependent manner with NS3.



 

Journal of Molecular Recognition

### NS3 or NS3 co-immobilized with NS4A

Since this study was performed using a full-length NS3 construct without fused or co-expressed NS4A, the effect of this cofactor on inhibitor binding could be investigated. NS3 is practically proteolytically inactive in the absence of NS4A (Failla *et al*., 1994), and such studies can therefore not be performed using an activity assay. A surface with both NS3 and NS4A increased the overall affinity for all studied protease inhibitors as compared to surfaces with NS3 alone. The high correlation between the two surfaces and with inhibition data from an enzyme inhibition assay or replicons in cell culture revealed that NS4A is not required for the binding of protease inhibitors and the number of components in the system could in principle be reduced. This is in agreement with previous findings on inhibitor and substrate stabilization of NS3 in the absence of NS4A (Barbato *et al*., 1999; Barbato *et al*., 2000; Gallo *et al*., 2009). Although NS3 without NS4A is a less relevant model system from an *in vivo* perspective, and resulted in lower affinities for inhibitors, omitting NS4A from interaction studies would still allow for relative measurements and inhibitor rankings. Faster dissociation rates, as observed in absence of NS4A, would increase the throughput for biosensor-based interaction analysis. Due to the lack of an efficient surface regeneration, this is a bottleneck. Moreover, this would avoid the risk of creating heterogeneous surfaces where free NS3 and free NS4A may be in a rate-limiting equilibrium with NS3-NS4A complexes on the surface. The binding of all inhibitors in the present study was affected by NS4A. NS4A thus appears to have a direct effect on the binding of inhibitors to NS3 and not only on catalysis. However, previous findings showed that inhibitors binding to the non-prime side of NS3 are less affected by the presence or absence of NS4A (Landro *et al*., 1997). This indicated that further studies might be required to evaluate whether a reduced component assay is applicable when comparing inhibitors of different classes.

### NS3 heterogeneity

The interaction between NS3 and NS4A, as well as that between NS3 and inhibitors, was clearly heterogeneous. In both cases, it was possible to distinguish a high-affinity interaction from a low-affinity interaction, their relative contributions to the overall affinity, and to determine the kinetic constants for both interactions. Heterogeneity in this type of analysis may be a consequence of the immobilization of a heterogeneous protein population or a heterogeneous immobilization of a homogeneous population. These experimental artefacts cannot be excluded, but are interpreted to be unlikely in light of the evidence for a mechanistically sound explanation.

The apparently low amount of functional NS3 on the surface suggests that the sensor surface consisted of both properly folded enzyme that interacted with ligands as expected, and a large fraction of improperly folded protein. This fraction may bind ligands in a well-defined but suboptimal way or completely non-specifically. However, it is unlikely that such interactions would be well described by a simple two-exponential model. Also, the affinity for the low-affinity interaction is higher than expected for non-specific interactions.

Therefore, the heterogeneity has been hypothesized to reflect interactions with two (or more) distinct conformations of the enzyme that are in slow (i.e. rate-limiting) equilibrium. Heterogeneous interactions of this type have previously been described for small molecule interactions (see for example Geitmann *et al*., 2006), and it is reasonable to assume that it is an intrinsic property of biomolecular interactions involving conformationally flexible proteins, such as NS3. The heterogeneity appears to be a general feature of the protein as it occurs irrespective if the ligand is NS4A or an inhibitor. Moreover, it is not induced by the binding of NS4A, although this interaction may possibly stabilize one of the forms. Also, the two interactions contributed approximately equally to the overall interactions, for both BILN 2061 and ITMN-191, and similarly for NS4A binding. It cannot at this stage be distinguished if the NS3–NS4A complex relevant for binding of inhibitors is only that represented by the high-affinity NS4A interaction, or if also the low affinity interaction is relevant.

It is tempting to speculate that the heterogeneity represents the two forms of NS3 that appears to exist during the membrane association process of NS3-4A (Brass *et al*., 2008). As suggested by the crystal structure of full length NS3, the helicase serves as a lid over the active site of the protease (Barbato *et al*., 1999), while a model of NS3 with a conformation with an open active site, resulting from an interaction between the helicase domain and the membrane surface has also been proposed (Brass *et al*., 2008). These two conformations are not incompatible, but may represent different conformations occurring at different stages of the replication of the viral genome. It is likely that they are in slow equilibrium and that they have different affinities for both NS4A and inhibitors. Further studies will be undertaken to explore this hypothesis, especially concerning the characteristics of the helicase and protease domains as well as their interplay with one another, which has been in focus lately (Dahl *et al*., 2007a, b; Beran and Pyle, 2008; Dahl *et al*., 2009).

## CONCLUSION

The development of a biosensor-based approach for studying interactions between full-length NS3 and an NS4A cofactor peptide as well as with protease inhibitors has not only provided mechanistic and kinetic details of these interactions, but also evidence for an inherent heterogeneity of NS3. It is expected that this method will contribute to a deepened understanding of the function of NS3 and its characteristics.

## Acknowledgements

We thank Anja Sandström, Eva Åkerblom and Robert Rönn at the Department of Medicinal Chemistry, Organic Pharmaceutical Chemistry, Uppsala University, Sweden for inhibitors 1–6 and Gunnar Lindeberg at the same department for the synthesis of NS4A. We also thank Boehringer-Ingelheim for their kind gift of BILN 2061 and the VIRGIL DrugPharm Team for VX 950. We thank GE Healthcare Life Science, Uppsala, Sweden for the opportunity to use the CM7 sensor chip. This work has been conducted with support from the VIRGIL European Union Network of Excellence.



  

## REFERENCES

Backman D, Monod M, Danielson UH. 2006. Biosensor-based screening and characterization of HIV-1 inhibitor interactions with Sap 1, Sap 2, and Sap 3 from Candida albicans. *J. Biomol. Screen.* **11**: 165–175.

Barbato G, Cicero DO, Cordier F, Narjes F, Gerlach B, Sambucini S, Grzesiek S, Matassa VG, De Francesco R, Bazzo R. 2000. Inhibitor binding induces active site stabilization of the HCV NS3 protein serine protease domain. *EMBO J.* **19**: 1195–1206.

Barbato G, Cicero DO, Nardi MC, Steinkühler C, Cortese R, De Francesco R, Bazzo R. 1999. The solution structure of the N-terminal proteinase domain of the hepatitis C virus (HCV) NS3 protein provides new insights into its activation and catalytic mechanism. *J. Mol. Biol.* **289**: 371–384.

Beran RK, Lindenbach BD, Pyle AM. 2009. The NS4A protein of hepatitis C virus promotes RNA-coupled ATP hydrolysis by the NS3 helicase. *J. Virol.* **83**: 3268–3275.

Beran RK, Pyle AM. 2008. Hepatitis C viral NS3-4A protease activity is enhanced by the NS3 helicase. *J. Biol. Chem.* **283**: 29929–29937.

Bianchi E, Urbani A, Biasiol G, Brunetti M, Pessi A, De Francesco R, Steinkühler C. 1997. Complex formation between the hepatitis C virus serine protease and a synthetic NS4A cofactor peptide. *Biochemistry* **36**: 7890–7897.

Brass V, Berke JM, Montserret R, Blum HE, Penin F, Moradpour D. 2008. Structural determinants for membrane association and dynamic organization of the hepatitis C virus NS3-4A complex. *Proc. Natl Acad. Sci. USA* **105**: 14545–14550.

Dahl G, Gutierrez Arenas O, Danielson UH. Hepatitis C virus NS3 protease is activated by low concentrations of protease inhibitors. *Biochemistry* **8**: 11592–11602.

Dahl G, Sandström A, Åkerblom E, Danielson UH. 2007a. Resistance profiling of hepatitis C virus protease inhibitors using full-length NS3. *Antivir. Ther.* **12**: 733–740.

Dahl G, Sandström A, Åkerblom E, Danielson UH. 2007b. Effects on protease inhibition by modifying of helicase residues in hepatitis C virus nonstructural protein 3. *FEBS J.* **274**: 5979–5986.

Eckart MR, Selby M, Masiarz F, Lee C, Berger K, Crawford K, Kuo C, Kuo G, Houghton M, Choo QL. 1993. The Hepatitis C virus encodes a serine protease involved in processing of the putative nonstructural proteins from the viral polyprotein precursor. *Biochem. Biophys. Res. Commun.* **192**: 399–406.

Failla C, Tomei L, De Francesco R. 1994. Both NS3 and NS4A are required for proteolytic processing of hepatitis C virus nonstructural proteins. *J. Virol.* **68**: 3753–3760.

Feld JJ, Hoofnagle JH. 2005. Mechanism of action of interferon and ribavirin in treatment of hepatitis C. *Nature* **436**: 967–972.

Flores MV, Strawbridge J, Ciaramella G, Corbau R. 2009. HCV-NS3 inhibitors: Determination of their kinetic parameters and mechanism. *Biochim. Biophys. Acta* **1794**: 1441–1448.

Gallo M, Pennestri M, Bottomley MJ, Barbato G, Eliseo T, Paci M, Narjes F, De Francesco R, Summa V, Koch U, Bazzo R, Cicero DO. 2009. Binding of a noncovalent inhibitor exploiting the S′ region stabilizes the hepatitis C virus NS3 protease conformation in the absence of cofactor. *J. Mol. Biol.* **385**: 1142–1155.

Geitmann M, Danielson UH. 2004. Studies of substrate-induced conformational changes in human cytomegalovirus protease using optical biosensor technology. *Anal. Biochem.* **332**: 203–214.

Geitmann M, Unge T, Danielson UH. 2006. Interaction kinetic characterization of HIV-1 reverse transcriptase non-nucleoside inhibitor resistance. *J. Med. Chem.* **49**: 2375–2387.

Huber W, Mueller F. 2006. Biomolecular interaction analysis in drug discovery using surface plasmon resonance technology. *Curr. Pharm. Des.* **12**: 3999–4021.

Kim DW, Gwack Y, Han JH, Choe J. 1995. C-terminal domain of the hepatitis C virus NS3 protein contains an RNA helicase activity. *Biochem. Biophys. Res. Commun.* **215**: 160–166.

Kim JL, Morgenstern KA, Lin C, Fox T, Dwyer MD, Landro JA, Chambers SP, Markland W, Lepre CA, O'Malley ET, Harbeson SL, Rice CM, Murcko MA, Caron PR, Thomson JA. 1996. Crystal structure of the hepatitis C virus NS3 protease domain complexed with a synthetic NS4A cofactor peptide. *Cell* **87**: 343–355.

Landro JA, Raybuck SA, Luong YP, O'Malley ET, Harbeson SL, Morgenstern KA, Rao G, Livingston DJ. 1997. Mechanistic role of an NS4A peptide cofactor with the truncated NS3 protease of hepatitis C virus: elucidation of the NS4A stimulatory effect via kinetic analysis and inhibitor mapping. *Biochemistry* **36**: 9340–9348.

Lin C, Lin K, Luong YP, Rao BG, Wei YY, Brennan DL, Fulghum JR, Hsiao HM, Ma S, Maxwell JP, Cottrell KM, Perni RB, Gates CA, Kwong AD. 2004. *In vitro* resistance studies of hepatitis C virus serine protease inhibitors, VX-950 and BILN 2061: structural analysis indicates different resistance mechanisms. *J. Biol. Chem.* **279**: 17508–17514.

Llinàs-Brunet M, Bailey M, Déziel R, Fazal G, Gorys V, Goulet S, Halmos T, Maurice R, Poirier M, Poupart M, Rancourt J, Thibeault D, Wernic D, Lamarre D. 1998. Studies on the C-terminal of hexapeptide inhibitors of the hepatitis C virus serine protease. *Bioorg. Med. Chem. Lett.* **8**: 2719–2724.

Lohmann V, Körner F, Koch J, Herian U, Theilmann L, Bartenschlager R. 1999. Replication of subgenomic hepatitis C virus RNAs in a hepatoma cell line. *Science* **285**: 110–113.

Markgren PO, Schaal W, Hämäläinen M, Karlén A, Hallberg A, Samuelsson B, Danielson UH. 2002. Relationships between structure and interaction kinetics for HIV-1 protease inhibitors. *J. Med. Chem.* **45**: 5430–5439.

Nordström H, Gossas T, Hämäläinen M, Källblad P, Nyström S, Wallberg H, Danielson UH. 2008. Identification of MMP-12 inhibitors by using biosensor-based screening of a fragment library. *J. Med. Chem.* **51**: 3449–3459.

Poliakov A, Hubatsch I, Shuman CF, Stenberg G, Danielson UH. 2002. Expression and purification of recombinant full-length NS3 protease-helicase from a new variant of Hepatitis C virus. *Protein Expr. Purif.* **25**: 363–371.

Poliakov A, Sandström A, Åkerblom E, Danielson UH. 2007. Mechanistic studies of electrophilic protease inhibitors of full length hepatic C virus (HCV) NS3. *J. Enz. Inhib. Med. Chem.* **22**: 191–199.

Rajagopalan R, Misialek S, Stevens S, Myszka D, Brandhuber B, Ballard J, Andrews S, Seiwert S, Kossen K. 2009. Inhibition and binding kinetics of the hepatitis C virus NS3 protease inhibitor ITMN-191 reveals tight binding and slow dissociative behavior. *Biochemistry* **48**: 2559–2568.

Rönn R, Gossas T, Sabnis YA, Daoud H, Åkerblom E, Danielson UH, Sandström A. 2007. Evaluation of a diverse set of potential P1 carboxylic acid bioisosteres in hepatitis C virus NS3 protease inhibitors. *Bioorg. Med. Chem.* **15**: 4057–4068.

Rönn R, Sabnis YA, Gossas T, Åkerblom E, Danielson UH, Hallberg A, Johansson A. 2006. Exploration of acyl sulfonamides as carboxylic acid replacements in protease inhibitors of the hepatitis C virus full-length NS3. *Bioorg. Med. Chem.* **14**: 544–559.

Rönn R, Sandström A. 2008. New developments in the discovery of agents to treat hepatitis C. *Curr. Top. Med. Chem.* **8**: 533–562.

Seiwert SD, Andrews SW, Jiang Y, Serebryany V, Tan H, Kossen K, Rajagopalan PT, Misialek S, Stevens SK, Stoycheva A, Hong J, Lim SR, Qin X, Rieger R, Condroski KR, Zhang H, Do MG, Lemieux C, Hingorani GP, Hartley DP, Josey JA, Pan L, Beigelman L, Blatt LM. 2008. Preclinical characteristics of the hepatitis C virus NS3/4A protease inhibitor ITMN-191 (R7227). *Antimicrob. Agents Chemother.* **52**: 4432–4441.

Shepard CW, Finelli L, Alter MJ. 2005. Global epidemiology of hepatitis C virus infection. *Lancet Infect. Dis.* **5**: 558–567.

Shuman CF, Hämäläinen MD, Danielson UH. 2004a. Kinetic and thermodynamic characterization of HIV-1 protease inhibitors. *J. Mol. Recognit.* **17**: 106–119.

Shuman CF, Vrang L, Danielson UH. 2004b. Improved structure-activity relationship analysis of HIV-1 protease inhibitors using interaction kinetic data. *J. Med. Chem.* **47**: 5953–5961.

Summa V. 2005. VX-950 (Vertex/Mitsubishi). *Curr. Opin. Investig. Drugs* **6**: 831–837.

Tomei L, Failla C, Vitale RL, Bianchi E, De Francesco R. 1996. A central hydrophobic domain of the hepatitis C virus NS4A protein is necessary and sufficient for the activation of the NS3 protease. *J. Gen. Virol.* **77**: 1065–1070.

Urbani A, Biasiol G, Brunetti M, Volpari C, Di Marco S, Sollazzo M, Orru S, Piaz FD, Casbarra A, Pucci P, Nardi C, Gallinari P, De Francesco R, Steinkuhler C. 1999. Multiple determinants influence complex formation of the hepatitis C virus NS3 protease domain with its NS4A cofactor peptide. *Biochemistry* **38**: 5206–5215.

Yao N, Reichert P, Taremi SS, Prosise WW, Weber PC. 1999. Molecular views of viral polyprotein processing revealed by the crystal structure of the hepatitis C virus bifunctional protease-helicase. *Structure* **7**: 1353–1363.



 